Eur. Phys. J. B (2014) 87: 225
DOI: 10.1140/epjb/e2014-50422-8

THE EUROPEAN PHYSICAL JOURNAL B

Regular Article

Infection dynamics in structured populations with disease awareness based on neighborhood contact history

Lang Cao[a]

School of Information Science and Technology, Fudan University, Shanghai, 200433, P.R. China

Received 23 June 2014 / Received in final form 21 July 2014
Published online 1 October 2014 –

Abstract. In recent years, continuing efforts have been directed to revealing the effect of human behavioral responses in the spread of infectious diseases. In this paper, we propose an implementation mechanism of disease awareness via individual self-perception from neighborhood contact histories (NCHs), where each individual is capable of memorizing a sequence of his infectious contacts earlier time, and adaptively adjusting the contact rate with his neighboring individuals as a preventive strategy from risks of exposure to infection. Both analytical and numerical results show that the NCH-based self-perceived awareness is a simple, but efficient disease control measure, which can greatly reduce the outbreak size of infectious diseases. We further examine the effects of a centralized disease control measure, which corresponds, for comparison, to an NCH-independent and uniformly aroused disease awareness. We find our proposed strategy outperforms the centralized one in a much larger and more practical range of epidemiological parameters, which also highlight the importance of the NCH-based awareness information in guidance of the individual protective behavior against infectious diseases.

1 Introduction

In the past decade, human societies have suffered from more and more serious consequences of worldwide outbreaks of communicable diseases. Mathematical epidemic spreading models have caught a great deal of attention of researchers, and numerous attempts have been made to reduce the frequency and severity of large-scale epidemic outbreaks [1–17]. Quite recently, analytically tractable incorporations of human behavioral factors into mathematical models for epidemics are becoming increasingly popular (for a review see Ref. [18] and references therein), and understanding such behavioral effects on the spread of infectious diseases is fundamental to step in appropriate and efficient intervention strategies for disease outbreak control.

A typical example can be found in recent studies on disease awareness in infection dynamics [19], where a portion of susceptible individuals within an infectious population are conventionally assumed to be capable of obtaining the cognition of contagious threats, and these individuals are subsequently equipped with preventive behavioral intention (i.e., the disease awareness) to reduce the incidence rate of infection. Up to now, attention has been mainly placed on the following two methodological approaches: (i) the awareness-related information as an information diffusion process interplaying with the infection dynamics [19–25]; and (ii) the awareness-responsive behavior as a coevolving process of adaptive networks [26–34].

Despite the success of existing implementations, one issue that has received relatively little attention is on a wide class of memory-related mechanisms that incorporate non-Markovian effects into the spread of infectious diseases [35]. In this paper we propose a self-perceived mechanism for the disease awareness based on the neighborhood contact history (NCH), assuming that individuals can obtain a perception of awareness by memorizing the past contacts with other infectious neighbors, and accordingly adjust their contact rates to reduce risks from infection if any contacts with infective individuals in the neighborhood were detected and recorded in their memories.

An intuition behind this assumption is that the contact history often serves as a key criterion for suspecting the diagnosis in the epidemiology literature, sufficing to raise awareness among (susceptible) individuals having infectious contact histories. Such non-Markovian, memory-based effects have also been widely found in many socio-physical phenomena. For example, in opinion dynamics or evolutionary games, individuals are usually more apt to adopt more advantageous strategies or opinions of the past, which are, e.g., capable of resulting higher (accumulated) utilities [36–39]. Besides, another widely used engineering application of NCHs comes from the design of routing protocols for communication networks. Within the framework of some more sophisticated routing algorithms, every delivery node of the network can predict future contacts using the stored NCH in its buffered memory to optimize routing decisions [40–42].

[a] e-mail: fandyclang@gmail.com

The remainder of this paper is organized as follows. In Section 2, we explain our basic assumptions on an extended epidemic model equipped with the NCH-based disease awareness. In Section 3, we provide a theoretical analysis of our model using the mean-field approximation, and the obtained results on epidemic thresholds and outbreak sizes show that the NCH-based awareness plays an important role in controlling and reducing the prevalence of infectious diseases. To highlight the significance of the NCH-based disease awareness, we further compare our proposed strategy with the null model, in which the population disease awareness is assumed to be uniformly persisted under the guidance of some centralized mechanism, instead of replying on the local information of individual NCHs. Finally, Section 4 concludes the whole work.

2 Model description

Let us start to build our model by first introducing the classical Susceptible-Infected-Susceptible (SIS) epidemiological model. Consider a population of n individuals located at nodes of a contact network, and contacts for the spread of infection between individuals are described as links of the network. Each individual can only exist in one of two discrete states: susceptible ($\mathcal{S}$) or infected ($\mathcal{I}$), and the basic infection dynamics is formulated as a reaction-diffusion-decay process:

$$\mathcal{S} + \mathcal{I} \xrightarrow{\beta} 2\mathcal{I}, \mathcal{I} \xrightarrow{\mu} \mathcal{S},$$

where β is the contact rate, and μ is the recovery rate. Here the contact rate β describes how frequently two individuals are contacting with each other to cause potential spread of infection.

Next, we propose a self-perceived mechanism for the disease awareness based on neighborhood contact history (NCH), assuming that individuals can obtain a perception of awareness by memorizing the past contacts with other infectious neighbors, and accordingly adjust their contact rates to reduce the risk from infection if any contacts with infective individuals in the neighborhood were detected and recorded in their memories. To incorporate the effect of disease awareness, we assign each node v_i with an adjustable contact rate $\beta_i(t)$, at which node v_i makes contact with the neighboring nodes at time t, and the adaptation of β_i based on v_i's NCH is given by:

$$\beta_i(t) = \beta_{i0} \prod_{j \in \mathcal{N}_i} \prod_{h=1}^{\lfloor t/\Delta t \rfloor} [1 - w_i(h\Delta t) s_j(t - h\Delta t)], \quad (1)$$

where β_{i0} is the baseline contact rate of node v_i, $\mathcal{N}_i$ is the neighborhood set of all the nodes connected to v_i in the network, Δt is the time step size ($\lfloor \cdot \rfloor$ denotes the floor function), and $s_j(\tau)$ is the state-variable of node v_j, which equals to 1 if node v_j stayed infected at time τ and 0 otherwise.

Since equation (1) descriptive of the awareness mechanism plays a pivot role in our infection model, let us examine some support to the reality of our basic model assumption. First, the baseline contact rate β_{i0} can be thought of as some individual v_i's susceptibility to the infection with his/her routine interpersonal contact frequency in complete absence of disease awareness. Once aroused, the disease awareness will affect individual contact patterns so that this susceptibility of him/her is reduced. For example, because of the onset of an infectious disease of some family member Bob, Alice may accordingly decide to wear an illness-protective mask for herself. This awareness-related behavior can effectively cause, say, 50% reduce in her susceptibility. Additionally, if another one of Alice's friends, Charlie, has also caught the same infection, Alice may further upgrade her awareness level by reducing 50% her outdoor activities to avoid infection risks. Note that the extent which Alice's awareness-guided action works against the infection's susceptibility (e.g., a 50% reduce in β_{i0}) is parametrized by the corresponding weights $w_i(t)$ in equation (1). Therefore, her "equivalent" contact rate will be lowered to $\beta^{\text{Alice}} \to 25\% \times \beta_0^{\text{Alice}}$. It is a natural assumption that the effects of such disease awareness aroused by different neighbors accumulate in a multiplicative way, as we proposed. Here, we provisionally assume that the state-variables $s_j(t)$ of her neighboring individuals (Bob, Charlie, et al.) are available to Alice. This is also a reasonable assumption when the infection network corresponds to the household or other social and interpersonal relationships, or there is some identifiable infectious symptom for the community of patients[1].

Noting that the aroused awareness will be ultimately mitigated as the passage of time. Let us return to the above example. Alice will gradually forget to wear masks and recovers to her original frequency of outdoor activities, as long as there is no renewal of her awareness due to latter contacts with other infectious individuals. To embody this fading effect of individual memory, we adopt a decreasing sequence of positive coefficients $w_i(\tau)$ which weights the contribution of history information entered v_i's NCH τ time steps before. Specifically, throughout the rest of the paper, we set for all individuals

$$\beta_{i0} = \beta, w_i(\tau) = \epsilon e^{-\xi\tau}, \quad (2)$$

where ϵ is the parameter that adjusts the intensity of the disease awareness, and ξ indicates the decaying rate of individual memories. Here, we assume that each node has an infinite length of memory, but there is no memory of neighborhood contact events prior to time $t = 0$.

More precisely, the epidemiological process is specified as follows. Consider a completely susceptible popula-

[1] In some case of infectious individuals lacking identifiable symptoms, we need to address this problematic issue on the ambiguity of epidemiological states. In contrary to a binary version of our model (Eq. (1)), introduce a continuous-valued state-variable $s_j(t) \in [0, 1]$ as the state of individual v_j that can be perceived by others. Here, $s_j(t)$ can be interpreted as the expressibility of v_j, which equals to the conditional probability of being correctly perceived as "infected" given v_j in state $\mathcal{I}$. Infection expressibility could be of much practical interest, but is out of the scope of this paper.

tion, and initially, the epidemiological state of all individuals is set as $s_i(0) = 0$ for the entire population except one individual who is randomly selected as a seeded case of the infectious disease. Also, all individual memory is cleared at the beginning of the process, and the NCH is an empty sequence for all individuals at the initial time $t = 0$. To start the hth step, every individual first recalls his recorded NCH sequence by the end of the previous step (by the time $h\Delta t$), and he decides an adaptive contact rate $\beta_i(t)$ according to equation (1) for the future step $t = h\Delta t$. Once entering the next step, during the interval $[t, t + \Delta t)$ every susceptible individual contacts with his neighboring infected individuals at the contact rate $\beta_i(t)$ (i.e., such an infectious contact causing the spread of the disease ($\mathcal{S}+\mathcal{I} \to 2\mathcal{I}$) occurs with probability $\beta_i(t)\Delta t$), and successively, infected individuals undergo the recovery process ($\mathcal{I} \to \mathcal{S}$) at the recovery rate μ. Here we assume, for simplicity, that the updating of epidemiological states of all individuals is synchronous. At the end of time step $t + \Delta t$, each individual appends the very recent neighborhood contact information (i.e., states of his neighboring individuals $\{s_j(t)|j \in \mathcal{N}_i\}$) to his NCH sequence. Then, using equation (1) and this updated NCH information, he calculates $\beta_i(t + \Delta t)$ for the next step. This process is iterated sufficiently many times until the population arrives at a steady infectious density, which defines an outbreak size ρ_∞. Particularly, an eradication of the disease corresponds to $\rho_\infty = 0$.

3 Model solution

3.1 Homogeneous population structure

To visualize the impact of the NCH-based awareness on the spread of infectious diseases, we first simulate the preventive action of aware-bearing individuals during the spreading process among a homogeneously structured population. With different contact rates β and awareness intensities ϵ, the corresponding final outbreak sizes ρ_∞ are plotted in Figure 1, which shows that ρ_∞ decreases with the intervention of disease awareness, whereas the critical contact rate λ_c (i.e., the minimal value thereof that is required to sustain transmission and outbreak of the disease) stays unchanged for respective level of the disease awareness of individuals.

Next, we first present a mean-field analysis for the infection spreading process with NCH-based awareness in homogeneous populations, and then discuss the case of heterogeneity of connectivity between individuals in a later section. Let $\rho(t) = \sum_i s_i(t)/n$ be the relative density of infected nodes at time t, and substituting equation (2) into equation (1), we have the average contact rate to a limit of weak awareness intensity ($\epsilon \to 0$)

$$\bar{\beta}(t) = \beta \left[1 - \epsilon \langle k \rangle \sum_{h=1}^{\lfloor t/\Delta t \rfloor} e^{-\xi h \Delta t} \rho(t - h\Delta t)\right], \quad (3)$$

where $\langle k \rangle$ is the average degree, i.e., the individuals' average number of contacting neighbors in the network.

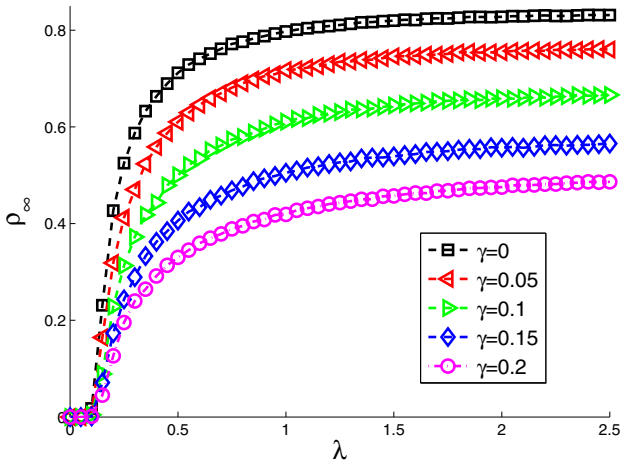

Fig. 1. Final outbreak size ρ_∞ as increasing functions of effective contact intensity λ ($=\beta/\mu$) with different effective awareness intensities γ ($=\epsilon/\xi$). The population structure is computer-generated by Erdős-Rényi random graph model [43]. Parameters are set as: network size $n = 10^3$, average degree $\langle k \rangle = 10$, disease recovery rate $\mu = 0.2$ (and changing contact rates β), memory decaying factor $\xi = 0.5$ (and changing awareness intensities ϵ), and time step $\Delta t = 1$. Each data point is obtained by averaging over 50 independent realizations.

Thus, we have the following rate equation for the infection dynamics:

$$\rho(t + \Delta t) = \rho(t) + \left\{-\mu\rho(t) + \bar{\beta}(t) \langle k \rangle \rho(t) [1 - \rho(t)]\right\} \Delta t.$$

Taking the limit $\Delta t \to 0$ leads to

$$\dot{\rho} = -\mu\rho + \beta \langle k \rangle \rho (1 - \rho) \left[1 - \epsilon \langle k \rangle \int_0^t e^{-\xi(t-\tau)} \rho(\tau) d\tau\right],$$

where the dot represents the time derivative, and going to the continuous limit, the summation term of equation (3) becomes $\phi(t) = \int_0^t e^{-\xi(t-\tau)} \rho(\tau) d\tau$ after a standard approximation. Differentiating $\phi(t)$ yields $\dot{\phi} = \rho - \xi\phi$, and at the equilibrium we have $\phi_\infty = \rho_\infty/\xi$. Substituting it into the above rate equation, we obtain the outbreak size ρ_∞ satisfying

$$0 = -\rho_\infty + \lambda \langle k \rangle \rho_\infty (1 - \rho_\infty) (1 - \gamma \langle k \rangle \rho_\infty), \quad (4)$$

for notional simplicity, here we introduce the effective contact intensity $\lambda = \beta/\mu$ as the ratio between the contact rate β and the recovery rate μ, and the effective awareness intensity $\gamma = \epsilon/\xi$ as the ratio between the disease awareness intensity ϵ and the memory decaying rate ξ.

Obviously, a trivial root of equation (4) is $\rho_\infty = 0$, whereas our main interest focuses on another non-trivial solution within the interval $(0, 1]$, which is given by:

$$(1 - \rho_\infty) (1 - \gamma \langle k \rangle \rho_\infty) = \frac{1}{\lambda \langle k \rangle}. \quad (5)$$

One can easily verify from equation (5) the critical contact rate $\lambda_{\text{crit}}^{\text{hom}} = 1/\langle k \rangle$, which is the same as the well-established epidemic threshold of SIS model on homogeneous networks in the absence of disease awareness [44].

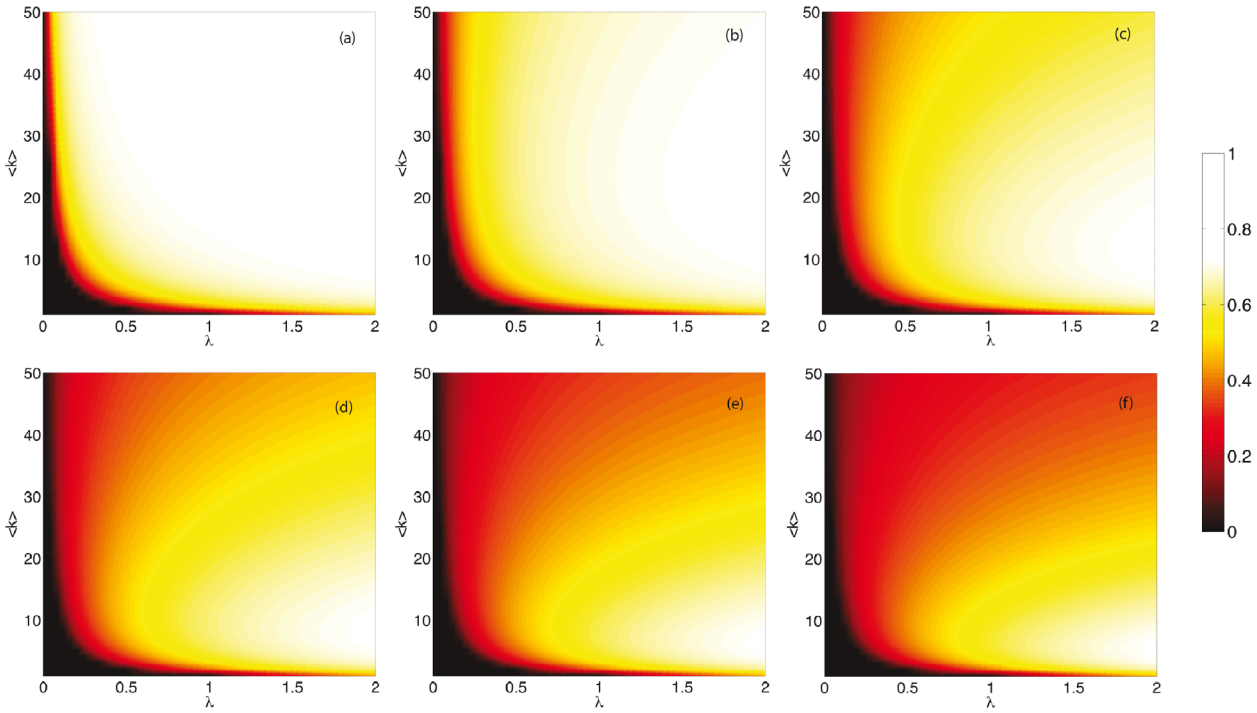

Fig. 2. Color-coded plot of the final outbreak size ρ_∞ as a function of effective contact intensity λ and average degree $\langle k\rangle$ under different effective awareness intensities: (a)–(f) $\gamma = 0, 0.05, 0.1, 0.15, 0.2, 0.25$, respectively. Each data point is obtained by averaging over 50 independent realizations on Erdős-Rényi random networks of size $n = 10^3$. Other parameters are set the same as those in Figure 1.

And if the contact rate exceeds the threshold ($\lambda > \lambda_{\rm crit}^{\rm hom}$), we approximately have

$$\rho_\infty = \frac{2}{1+\gamma\langle k\rangle + \sqrt{(1-\gamma\langle k\rangle)^2 + 4\gamma/\lambda}} \frac{\lambda - \lambda_{\rm crit}^{\rm hom}}{\lambda}. \quad (6)$$

Note that as the awareness intensity ϵ approaches zero ($\gamma \to 0$), equation (6) reduces to $\rho_\infty = (\lambda - \lambda_{\rm crit}^{\rm hom})/\lambda$ which yields the same result in the SIS model among homogeneous populations.

It should be pointed out that the above approximation (Eq. (6)) does not work for large $\langle k\rangle$, and more precisely, ρ_∞ is a non-trivial root (within the interval $(0, 1]$) of the following equation:

$$0 = -\mu\rho_\infty + (1-\rho_\infty)\left\{1 - \left[1 - \beta(1-\gamma\rho_\infty)^{\langle k\rangle}\right]^{\rho_\infty\langle k\rangle}\right\}. \quad (7)$$

To interpret equation (7), the effect of disease awareness is modeled by a decrement in the baseline contact rate β. From our model assumption (Eq. (1)), such awareness-related effect leads to a reduced contact rate $\beta^{\rm aware} \equiv \beta(1-\epsilon\phi)^{\langle k\rangle}$, noting that each individual has, on average, $\langle k\rangle$ neighbors among a homogeneous population, and accordingly reduces his contact rate to $(1-\epsilon\phi)$ times the baseline rate per each neighbor, where $\phi = \sum_{h=1}^{\lfloor t/\Delta t\rfloor} e^{-\xi h\Delta t}\rho(t-h\Delta t) \approx \int_0^t e^{-\xi(t-\tau)}\rho(\tau)d\tau$. Thus, the probability of an awareness-bearing individual being infected by one of his infectious neighbors $1-(1-\beta^{\rm aware})^{\rho\langle k\rangle}$, where $\rho\langle k\rangle$ is the expected number of infectious neighbors for each individual. Therefore, the rate equations become

$$\begin{aligned}\dot\rho &= -\mu\rho + (1-\rho)\left\{1 - \left[1-\beta(1-\epsilon\phi)^{\langle k\rangle}\right]^{\rho\langle k\rangle}\right\},\\ \dot\phi &= \rho - \xi\phi, \end{aligned} \quad (8)$$

the stationary condition of which comes to equation (7).

Since the outbreak size ρ_∞ has no explicit analytical form, we carry out extensive agent-based simulations on Erdős-Rényi random networks, as is shown in Figure 2. Simulation results reflect the impact of the effective awareness intensity γ and the average node degree $\langle k\rangle$ on the epidemic spreading, which also agree well with the numerical calculation results of equation (7). It shows that the outbreak size ρ_∞ decreases as γ is enhanced, and that the curve of ρ_∞ versus $\langle k\rangle$ presents an unimodal shape as is shown in the inset of Figure 3. Consider the following two extreme situations: (i) there are too few links in a sparse network to spread an infectious disease thereon; and (ii) there are dense links to raise a high-leveled disease aware among the population causing a substantial reduce in individual contact rates accordingly. Thus the topological structure in both cases inhibits the spread of infectious diseases on networks. Therefore, $\rho_\infty(k)$ shows a single peak with only one maximum value located at an intermediate average connectivity $\langle k\rangle^\star$ of networks. We further study how the effective contact rate λ and the effective awareness intensity γ affect the shapes of ρ_∞, and

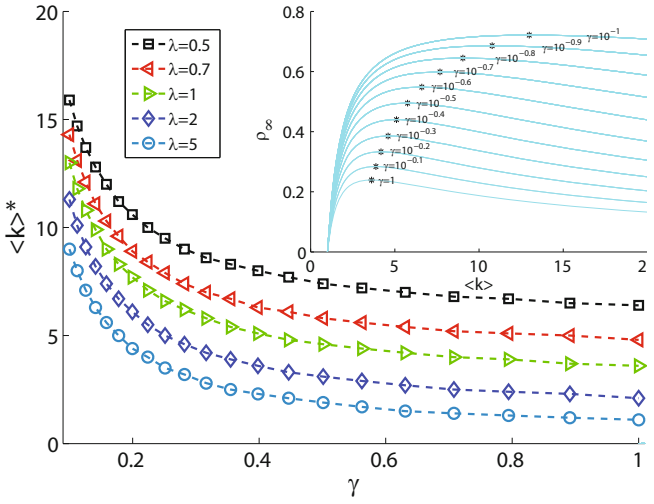

Fig. 3. Single-peak location $\langle k\rangle^\star$ of the final outbreak size ρ_∞ as a function of the average degree $\langle k\rangle$ of networks. With different effective contact λ and awareness intensities γ, we continuously tune the link probability p (i.e., the probability of establishing a link between each pair of nodes) of Erdős-Rényi random networks, on which we obtain outbreak sizes $\rho_\infty(p)$ by agent-based simulations. Then the $\langle k\rangle^\star = np^\star$ is identified by picking out the maxima $\rho_\infty(p^\star)$ of the simulation curves of $\rho_\infty(p)$, where $n = 10^3$ is the network size and other epidemiological parameters are set the same as those in Figure 2. Each data point is obtained by averaging over 50 independent realizations. (Inset) Verification of $\langle k\rangle^\star$ by exact solutions to equation (7). Each solid line corresponds to the exact roots of equation (7) as unimodal functions of $\langle k\rangle$ with various awareness intensities $\epsilon \in (0, 1]$ (here the effective contact intensity is set as $\lambda = 1$), and the symbol (asterisk) in each curve corresponds to the identified location $\langle k\rangle^\star$ from agent-based simulations, which is in a good agreement with the maxima location of numerical solutions to equation (7).

Figure 3 shows a positive (negative) correlation between λ (γ) and $\langle k\rangle^\star$, which is also consistent with the intuition.

3.2 Centralized versus decentralized control strategies

To highlight the role of NCH-based disease awareness as an individual self-protection strategy in the infection prevention and control, we further consider an alternative mechanism of disease awareness with random and/or uniform reduction of individual contact rates independent of the perceived NCH information. More precisely, given a "nominal" disease awareness level γ_0, we assume that the contact rate of each individual is reduced according to $\beta_i \to \beta_{i0}(1-\gamma_0)$, regardless of epidemiological states of his/her neighbors. Since the alternative mechanism acts as a non-informative counterpart of our proposed strategy, we refer to this randomized or mean-field case as our null model for comparison.

In an analogous manner, one can easily obtain the rate equation as

$$\dot{\rho}_0 = -\mu\rho_0 + (1-\rho_0)\left\{1-[1-\beta(1-\gamma_0)]^{\rho_0\langle k\rangle}\right\}, \quad (9)$$

the final outbreak size of which satisfies

$$0 = -\mu\rho_{0\infty} + (1-\rho_{0\infty})\left\{1-[1-\beta(1-\gamma_0)]^{\rho_{0\infty}\langle k\rangle}\right\}. \quad (10)$$

Here, we differentiate the null model by an additional suffix "zero". Note that the above expression for $\rho_{0\infty}$ follows by substituting a reduced contact rate $\beta_0^{\text{aware}} \equiv \beta(1-\gamma_0)$ into equation (7).

The null model also describes a common situation of disease awareness in many realistic scenarios. For example, with the help of mass media release of officially recognized surveillance reports, as well as disease warnings issued for the entire population, the individuals who even have no NCHs are also capable of obtaining safety-information on the status of an infectious disease, and accordingly taking some preventive measures [45]. The null model well corresponds to the centralized disease control via a population-leveled, uniformly aroused awareness, whereas the NCH-based mechanism can be thought of as a decentralized control strategy that heavily relies on local information and individual status of infection networks.

It should be noted that in the null model, a single parameter γ_0 completely controls the awareness level (and hence the final outbreak size), but under the NCH-based case, besides the intensity parameter γ, the awareness level also depends adaptively on prevalence of the infectious disease, i.e. ρ_∞ itself in turn influences individuals' awareness. Therefore, the average reduction in individual contact rates actually caused by the two methods under the same parameters $\gamma = \gamma_0$ is usually different, which may potentially hinder a completely faithful comparison. Next we make a provisional comparison between the two strategies by examining the corresponding final outbreak sizes, $\rho_\infty(\gamma)$ and $\rho_{0\infty}(\gamma_0)$, after exerting both awareness strategies with identical intensities on the same infection networks. Fortunately, under the situation of weak awareness intensities ($\gamma(\gamma_0) \ll 1$), this problematic issue is greatly mitigated. With the first-order approximation, we obtain from equations (10) and (7) the final outbreak sizes for both strategies

$$-1 + \lambda\langle k\rangle(1-\gamma_0)[1-\rho_{0\infty}(\gamma_0)] = 0, \quad (11)$$

$$-1 + \lambda\langle k\rangle[1-\gamma\langle k\rangle\rho_\infty(\gamma)][1-\rho_\infty(\gamma)] = 0. \quad (12)$$

Taking the limit $\gamma_0(\gamma) \to 0$ yields

$$\rho_{0\infty}(0) = \rho_\infty(0) = 1 - \frac{1}{\lambda\langle k\rangle}, \quad (13)$$

where $\rho_\infty(0)[\rho_{0\infty}(0)]$ stands for the awareness-absent outbreak size in the original infection network. Differentiating equations (11) and (12) with respect to $\gamma_0(\gamma)$ at the origin, we have

$$\rho'_{0\infty}(0) = -\frac{1}{\lambda\langle k\rangle}, \quad \rho'_\infty(0) = -\frac{1}{\lambda}\left(1-\frac{1}{\lambda\langle k\rangle}\right). \quad (14)$$

Therefore, under the assumption of weak awareness intensity, the condition that our NCH-based strategy is superior to the null model is given by

$$\rho'_\infty(0) < \rho'_{0\infty}(0) \Rightarrow \lambda > \lambda_{\text{crit}} = \frac{1}{\langle k\rangle - 1}, \quad (15)$$

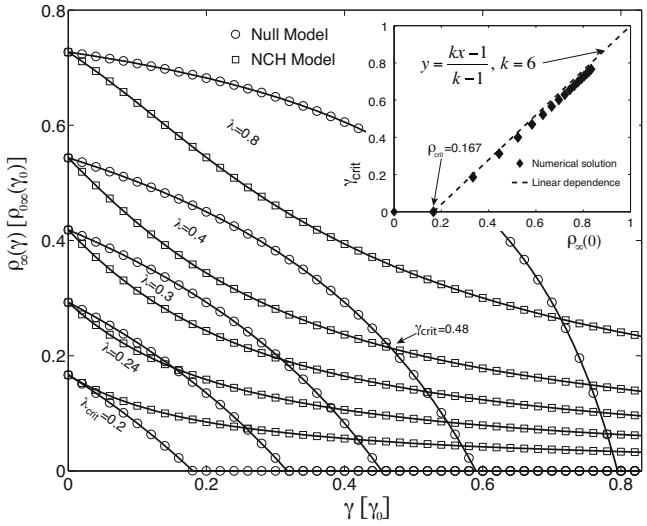

Fig. 4. Comparison of the NCH-based disease control strategy with the null model under different effective contact intensities and effective [centralized] awareness intensities $\gamma[\gamma_0]$. The average degree of random networks is set as $\langle k\rangle = 6$. The curves correspond to numerically exact solutions to implicit functions $\rho_\infty(\gamma)$ and $\rho_{0\infty}(\gamma_0)$ from equations (7) and (10). The condition equation (15) gives the critical contact intensity $\lambda_{\rm crit} = \frac{1}{\langle k\rangle - 1} = 0.2$, which corresponds to the situation of two curves being tangent at $(0, \rho^{\infty}_{\rm crit})$ with $\rho^{\infty}_{\rm crit} = \frac{1}{\langle k\rangle} \approx 0.167$. (Inset) A perfect linear dependence of numerical values for awareness intensity threshold $\gamma_{\rm crit}$ (see text) on awareness-absent outbreak sizes $\rho_\infty(0)$. The dashed line corresponds to the approximation relation equation (17). Other topological and epidemiological parameters are set the same as those in Figure 1.

which indicates that only a very narrow parameter range of the effective contact rate $\lambda \in]\frac{1}{\langle k\rangle}, \frac{1}{\langle k\rangle - 1}[$ guarantees that the centralized disease control strategy will outperform the decentralized one, as is shown in Figure 4. Note that epidemiological parameters of many real-world, globally-spread diseases are shown to be obviously above their thresholds[2], in which case it highlights the value of NCH information in guiding the individual behavioral response to infectious diseases, particularly when realizing a high intensity of disease awareness is unaffordable because of a large cost.

Besides, combining with equation (13), we can rewrite the condition equation (15) as

$$\rho_\infty(0) > \frac{1}{\langle k\rangle}, \tag{16}$$

implying a minimal prevalence degree of the disease that is required to maintain a comparable awareness level as the centralizedly controlled disease awareness in homogeneous populations.

It is also interesting to point out that the above condition bears a close resemblance to the epidemic threshold on homogeneous networks in form of $\lambda^{\rm hom}_{\rm crit} = 1/\langle k\rangle$. We shall see in later discussions that the quantity $\rho_\infty(0)$ plays a key role (Eq. (17)) in determining the effect of decentralized control strategy in our NCH-based model compared to that in the null cases.

At the other extreme, note that a large awareness intensity under the null model will eradicate the disease, since as γ_0 increases, individuals will be equivalently disconnected with each other (taking a limit $\gamma_0 \to 1$ in Eq. (10), we have $\rho_{0\infty}(\gamma_0) \to 0$). However, we have recognized that the NCH-based awareness does not change the epidemic threshold and hence $\rho_\infty(\gamma)$ stays positive, no matter how intense the disease awareness is aroused. Therefore, we find a critical intensity $\gamma = \gamma_0 = \gamma_{\rm crit}$, beyond which the centralized awareness strategy starts to be more advantageous owed to a substantial reduce in the epidemic threshold it causes.

Note that the threshold value of $\gamma_{\rm crit}$ sensibly increases as the effective contact rate λ increases. It should be noticed that a large awareness intensity can usually be costly. For example, when $\lambda = 0.4$, a centralized disease awareness at the threshold level $\gamma_{\rm crit} \approx 0.48$ (see Fig. 4). It means that nearly a half of links are required to be closed or "removed" from the original network, which could be hardly achieved in real-world, feasible disease control strategies. It also validates the effectiveness and efficiency of our NCH-based awareness strategy in a practical parameter range with relatively high infection risks ($\lambda > \lambda_{\rm crit}$) but comparatively low awareness intensities ($\gamma < \gamma_{\rm crit}$).

Unlike the condition equation (15) for $\lambda_{\rm crit}$, the analytical value of $\gamma_{\rm crit}$ is hard to find from implicit functions equations (7) and (10). But employing numerical solutions, we find $\gamma_{\rm crit}$ perfectly linearly related to the awareness-absent outbreak sizes, $\rho_\infty(0)$, as is shown in the inset of Figure 4. More precisely, the critical value for the awareness intensity $\gamma_{\rm crit}$ is approximately given by

$$\gamma_{\rm crit} = \begin{cases} 0, & \rho_\infty \le \frac{1}{\langle k\rangle} \\ \frac{\rho_\infty \langle k\rangle - 1}{\langle k\rangle - 1}, & \rho_\infty > \frac{1}{\langle k\rangle} \end{cases} \tag{17}$$

where $\langle k\rangle$ is the average degree of the network, and $\rho_\infty(0)$ is the final outbreak size thereof with null disease awareness.

3.3 Heterogeneous population structure

Next, let us move to non-homogeneous population structures, taking into account fluctuations in the number of acquaintance individuals in many real social networks, which typically exhibit the so-called scale-free feature with heterogeneous degree distributions obeying a power law, $p_k \sim k^{-\upsilon}$ with a scale-invariant exponent $\upsilon \in (2, 3]$. Similarly, we have the following rate equations neglecting degree correlations

$$\dot\rho_k = -\mu\rho_k + \beta k \Theta (1 - \rho_k) \left[1 - \epsilon k \int_0^t e^{-\xi(t-\tau)} \Theta(\tau) d\tau\right],$$

[2] E.g., the 2003 Severe Acute Respiratory Syndrome (SARS) estimated to have a basic reproductive number $\mathcal{R}_0 \in [2, 5]$, which is deemed significantly higher than unity [46].

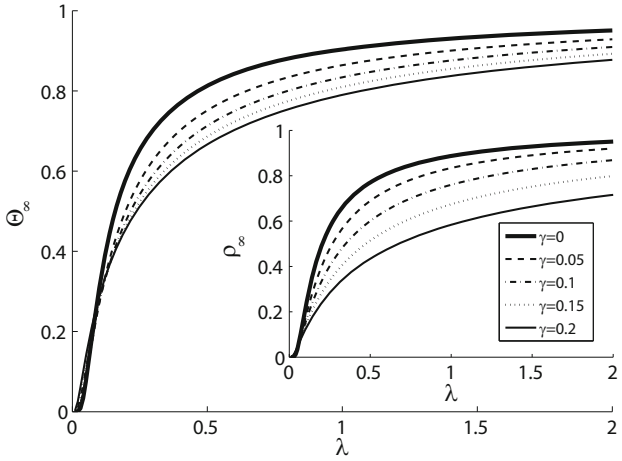

Fig. 5. Analytically predicted Θ_∞ (by Eq. (20)) and final outbreak size ρ_∞ (inset) as a function of effective contact intensity λ with different effective awareness intensities $\gamma = 0$ (thick solid line), 0.05 (dashed line), 0.1 (dash-dotted line), 0.15 (dotted line), and 0.2 (thin solid lind). One can easily verify that equation (20) reduces to the existing result $\Theta_\infty^{\gamma\to 0} = [\lambda m(e^{1/\lambda m} - 1)]^{-1}$ to a limit of weak intensity of awareness ($\epsilon \to 0$), which corresponds to the thick solid line ($\gamma = 0$). (Inset) Analytically predicted final outbreak size (by the mean-field rate equations Eq. (18)) ρ_∞ as a function of effective contact intensity λ. The population structure is computer-generated by Barabási-Albert scale-free network model [47] with the node size $n = 10^3$ and the minimal node degree $m = 5$. The epidemiological parameters are set the same as those of Figure 1.

where ρ_k is the relative infected density among nodes with degree k, $\Theta = \sum_k kp_k\rho_k / \sum_{k'} k'p_{k'}$ is the probability of reaching an infectious node along a randomly selected link. Similarly, with the variable substitution $\phi(t) = \int_0^t e^{-\xi(t-\tau)}\Theta(\tau)d\tau$, we obtain

$$\dot{\rho}_k = -\mu\rho_k + \beta k\Theta\left(1-\rho_k\right)\left(1-\epsilon k\phi\right), \dot{\phi} = \Theta - \xi\phi, \quad (18)$$

and the stationary condition of equation (18) is given by[3]

$$\rho_{k\infty} = \frac{\lambda k\Theta_\infty\left(1-\gamma k\Theta_\infty\right)}{1+\lambda k\Theta_\infty\left(1-\gamma k\Theta_\infty\right)}, \quad (19)$$

where $\Theta_\infty = \sum_k kp_k\rho_{k\infty} / \sum_{k'} k'p_{k'}$. Therefore, we obtain the epidemic threshold from this self-consistent relation of Θ_∞

$$\frac{\partial}{\partial\Theta_\infty}\sum_k \frac{kp_k}{\langle k\rangle}\frac{\lambda k\Theta_\infty\left(1-\gamma k\Theta_\infty\right)}{1+\lambda k\Theta_\infty\left(1-\gamma k\Theta_\infty\right)}\bigg|_{\Theta_\infty=0} \geq 1,$$

and we revisits the well-known epidemic threshold $\lambda_c^{\text{het}} = \langle k\rangle/\langle k^2\rangle$ as the same as that in the absence of awareness [48], where $\langle k\rangle = \sum_k kp_k$ is the average degree, and $\langle k^2\rangle = \sum_k k^2p_k$ is the second moment of the degree distribution, which reflects the fluctuation in numbers of neighborhood contacts (adjacent links) for different nodes in the network.

Next, we show the impact of awareness on controlling the prevalence of infectious diseases by calculateingthe final outbreak size ρ_∞ under a given awareness intensity. Straightforwardly, it follows from equation (19) that, compared to the situation without awareness, the introduction of a positive intensity ($\epsilon > 0$) of disease awareness can decrease the values of Θ_∞, $\rho_{k\infty}$, and hence the outbreak size ρ_∞ as well.

However, it has difficulty finding the explicit and exact solution to equation (19) given an arbitrary degree distribution of networks. Especially, as a standard model of network topologies capturing the heterogeneity of connectivity patterns, we concentrate on Barabási-Albert scale-free networks, whose degree distribution reads a power law $p_k \sim k^{-\upsilon}$ with the exponent $\upsilon = 3$. From the self-consistent relation with the assumption of weak awareness intensity, we approximately obtain after some calculations (see Appendix A)

$$\Theta_\infty = \frac{r_1-1}{\gamma m}\left[e^{\frac{r_1-r_2}{(\lambda r_1+\gamma)m}} - 1\right]^{-1}, \quad (20)$$

where m is the minimum degree of the network and $r_{1,2} = \frac{1\pm\sqrt{1+4\gamma/\lambda}}{2}$.

Based on equation (20), we can use (without proof) the following approximation relation to estimate the outbreak size

$$\rho_\infty \sim e^{\frac{r_1-r_2}{(\lambda r_1+\gamma)m}}, \quad (21)$$

noting that if the disease awareness is absent ($\gamma \to 0$), it revisits the well-known result $\rho_\infty \sim e^{1/\lambda m}$ [44]. As is shown in Figure 6, we numerically verify the approximate result on the final outbreak size, which is close to exact solutions. The numerical results obtained by agent-based simulations are also plotted in Figure 7, which provides a more comprehensive view of the effect of our NCH-based awareness mechanism on controlling the prevalence of infectious diseases.

To further examine how contact patterns affect final endemic prevalence, we observe the individual incidence rate (i.e., the probability of being infected per unit time), which describes how likely an individual is infected by others, as is shown in Figure 8. Under the mean-field approximation, the average incidence rate of individuals with degree k is given by $\alpha_{k\infty} = [1-\beta(1-\gamma\Theta_\infty)^k]^{k\Theta_\infty}$. We also numerically show that those hub-like individuals – who have a large number of neighbors – usually evolve to a sharpened contact rate (Fig. 8), because a large amount of infectious contacts as their NCH information are gathered to arise a high-leveled disease awareness. This could be analogous to the targeted immunization strategy of infection networks [49], and as a result, the most likely

[3] Subject to a possible diverging maximum node degree in some situations of infinite networks, the infection dynamics (Eq. (18)) can be, analogous to equation (8), rewritten as $\dot{\rho}_k = -\mu\rho_k + (1-\rho_k)\{1-[1-\beta(1-\epsilon\phi)^k]^{k\Theta}\}, \dot{\phi} = \Theta - \xi\phi$. Thus, the stationary condition reads $\phi_\infty = \xi^{-1}\Theta$, and $\rho_{k\infty} = 1 - \{1 + \mu^{-1} - \mu^{-1}[1-\beta(1-\gamma\Theta_\infty)^k]^{k\Theta_\infty}\}^{-1}$, the first-order expansion of which is consistent with equation (19). Note that the epidemic threshold is derived from the instability condition of the self-consistent equation with respect to Θ_∞ at the origin point, therefore, this first-order approximation has no influence on the result of λ_c^{het}.

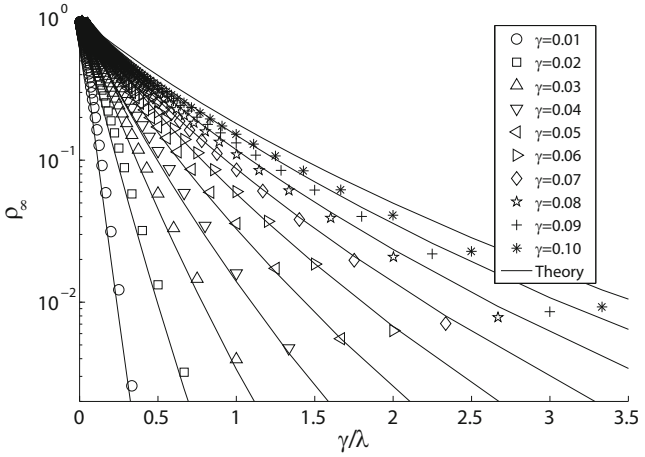

Fig. 6. Semi-logarithmic plot of analytically predicted outbreak size ρ_∞ as a function of the ratio $a = \gamma/\lambda$ between the effective awareness γ and the effective contact intensity λ. The symbols in the plot (e.g., boxes, triangles, etc.) correspond to values of ρ_∞ with different parameter pairs $(\gamma, \lambda) \in (0, 0.1] \times (0, 2]$, respectively, where the exact solutions to the self-consistent equation with respect to Θ_∞ are numerically solved and inserted into equation (19) to calculate $\rho_\infty = \sum_k p_k \rho_{k\infty}$. The solid lines correspond to the first order approximation relation $\rho_\infty \approx \exp\left[(r_1 - r_2)/\lambda m\,(a + r_1)\right]$ with $r_{1,2} = 1/2 \pm \sqrt{1 + 4a}/2$, which agree well with the exact solutions. Both topological and epidemiological parameters are set the same as those of Figure 5.

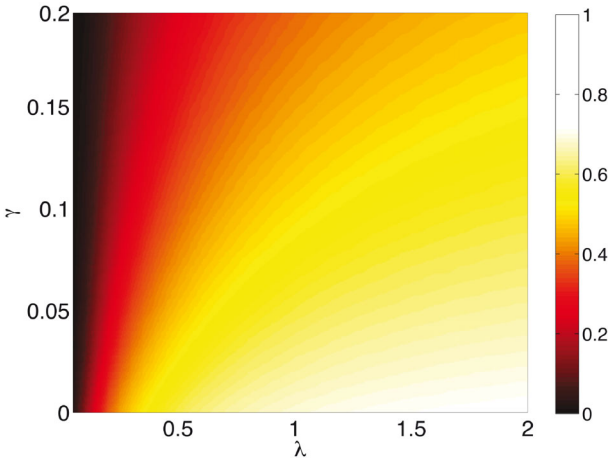

Fig. 7. Color-coded plot of the final outbreak size ρ_∞ as a function of effective contact intensity λ and effective awareness intensity γ. Both topological and epidemiological parameters are set the same as those of Figure 5. Each data point is averaged over 50 independent realizations.

infected individuals typically have, on average, an intermediate number of neighbors in heterogeneous networks, which is also consistent with our previous results of homogeneous networks (see Fig. 3).

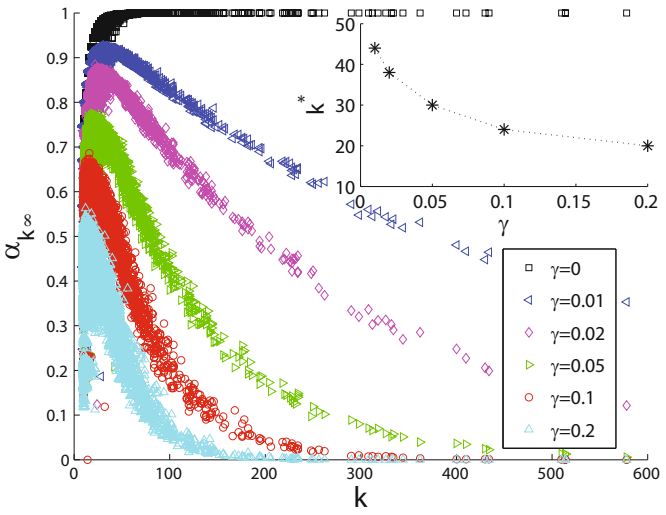

Fig. 8. Incidence rate of infection $\alpha_{k\infty}$ as unimodal functions of individual node degree k in steady endemic states. (Inset) The degrees $k^\star$ of individuals with the highest average incidence rate $\alpha_{k^\star}$. Parameters are set as: network size $n = 10^4$, average degree $\langle k \rangle = 10$, and effective contact intensity $\lambda = 1$.

4 Conclusion

In this paper, we have proposed a memory-based mechanism for implementing disease awareness in the epidemic spreading on networks, where the neighborhood contact information is utilized by individuals to estimate risks from being infected, and accordingly, a preventive strategy is adopted based on these neighborhood contact histories of individuals. The proposed strategy is very simple: the more frequently and recently an individual has encountered with infectious individuals, the less likely he will contact with others, i.e., the perceived disease awareness from the individual's NCH results in a decrement in his contact rate to reduce the risk of exposure.

In our devised framework, active contacts (between infectious spreaders and susceptible spreadees) are memorized by those susceptible individuals, which cause a self-isolation-like effect due to the disease awareness mechanism. Within a practical range of relatively low awareness intensities, our NCH-based decentralized strategy are more advantageous than the centralized one in mitigating the final outbreak size of the disease, unless its epidemiological parameter stays at a very slightly supercritical level. Our findings also highlight the significance of the NCH-information in adaptive mechanisms of the disease awareness. Besides, there are many other conceivable strategies of utilizing individual memories to guide human behavioral response to better protect against threats from infectious diseases. These issues deserve further study.

This work was partially supported by Research Program KFKT-2012101 from Key Laboratory of Universal Wireless Communications (Beijing University of Posts and Telecommunications), Ministry of Education, People's Republic China, and the National Natural Science Foundation (No. 61304156).

Appendix A: The derivation of Θ_∞ for Barabási-Albert scale-free networks

In the Appendix we present a detailed derivation of the approximate solution (Eq. (20)) to the following self-consistent equation with respect to Θ_∞

$$\Theta_\infty = \sum\nolimits_k \frac{kp_k}{\langle k\rangle} \frac{\lambda k\Theta_\infty\,(1-\gamma k\Theta_\infty)}{1+\lambda k\Theta_\infty\,(1-\gamma k\Theta_\infty)}, \tag{A.1}$$

where the node degree distribution of a Barabási-Albert scale-free network is given by $p_k \sim k^{-\upsilon}$ with the power-law exponent $\upsilon = 3$.

To facilitate the computation, we regard the degree distribution as a continuous function $p(k) = 2m^2/k^3$ on an interval $[k_{\min}, k_{\max}]$, where $k_{\min}$ and $k_{\max}$ are the maximum and minimum node degree of the network, respectively, and the constant factor $m = (k_{\min}^{-2} - k_{\max}^{-2})^{-1/2}$ works for normalization. Therefore we have the average degree $\langle k\rangle$

$$\langle k\rangle = \int_{k_{\min}}^{k_{\max}} kp(k)dk = \int_{k_{\min}}^{k_{\max}} \frac{2m^2}{k^2}dk = 2\frac{k_{\min}^{-1} - k_{\max}^{-1}}{k_{\min}^{-2} - k_{\max}^{-2}},$$

and substituting into equation (A.1) yields

$$\Theta_\infty = \frac{\lambda\Theta_\infty}{k_{\min}^{-1} - k_{\max}^{-1}} \int_{k_{\min}}^{k_{\max}} \frac{dk}{k} \frac{1-\gamma k\Theta_\infty}{1+\lambda k\Theta_\infty\,(1-\gamma k\Theta_\infty)}.$$

With variable replacement $y = 1-\gamma k\Theta_\infty$ for the integration part, the self-consistent equation comes to

$$\begin{aligned}\frac{k_{\min}^{-1} - k_{\max}^{-1}}{\lambda} &= \int_{1-\gamma k_{\max}\Theta_\infty}^{1-\gamma k_{\min}\Theta_\infty} \frac{dy}{(y-1)} \frac{ay}{y^2-y-a} \\ &= \ln\frac{k_{\max}}{k_{\min}} + \frac{a+r_1}{r_1-r_2}\ln\frac{\gamma k_{\min}\Theta_\infty + r_1 - 1}{\gamma k_{\max}\Theta_\infty + r_1 - 1} \\ &\quad - \frac{a+r_2}{r_1-r_2}\ln\frac{1-r_2-\gamma k_{\min}\Theta_\infty}{1-r_2-\gamma k_{\max}\Theta_\infty},\end{aligned} \tag{A.2}$$

where $a = \gamma/\lambda$ and $r_{1,2} = \frac{1\pm\sqrt{1+4a}}{2}$. Here, we used the following identity relation

$$\frac{ax}{(x-1)(x^2-x-a)} = \frac{A}{x-1} + \frac{B}{x-r_1} + \frac{C}{x-r_2},$$

with coefficients $A = -1$, $B = \frac{a+r_1}{r_1-r_2}$ and $C = -\frac{a+r_2}{r_1-r_2}$.

To make further simplification, we rewrite equation (A.2) as

$$\begin{aligned}\frac{k_{\min}^{-1} - k_{\max}^{-1}}{\lambda} &= \frac{a+r_1}{r_1-r_2}\ln\frac{\gamma\Theta_\infty + k_{\min}^{-1}(r_1-1)}{\gamma\Theta_\infty + k_{\max}^{-1}(r_1-1)} \\ &\quad - \frac{a+r_2}{r_1-r_2}\ln\frac{k_{\min}^{-1}(1-r_2) - \gamma\Theta_\infty}{k_{\max}^{-1}(1-r_2) - \gamma\Theta_\infty},\end{aligned}$$

and under the assumption of weak awareness intensity $\epsilon \ll 1$, the second term in the rhs expression can be neglected, since it is an infinitesimal of higher order than the first term. Thus equation (A.2) simplifies to

$$\frac{k_{\min}^{-1} - k_{\max}^{-1}}{\lambda} = \frac{a+r_1}{r_1-r_2}\ln\frac{\gamma\Theta_\infty + k_{\min}^{-1}(r_1-1)}{\gamma\Theta_\infty + k_{\max}^{-1}(r_1-1)}.$$

Taking the limit $k_{\max}\to\infty$, we have

$$\frac{1}{\lambda m} = \frac{a+r_1}{r_1-r_2}\ln\left[1 + \frac{r_1-1}{\gamma m\Theta_\infty}\right], \tag{A.3}$$

noting that the normalization constant $m = k_{\min}$ reduces to be the minimum degree of the network. Thus from equation (A.3) one can readily obtain

$$\Theta_\infty = \frac{r_1-1}{\gamma m}\left[e^{\frac{r_1-r_2}{\lambda m(a+r_1)}} - 1\right]^{-1}, \tag{A.4}$$

which is the same as equation (20).

References

1. N.T.J. Bailey, *The Mathematical Theory of Infectious Diseases and its Applications* (Griffin, London, 1975)
2. R.M. Anderson, R.M. May, *Infectious diseases of humans: dynamics and control* (Oxford University Press, Oxford, 1991)
3. R. Pastor-Satorras, A. Vespignani, Phys. Rev. E **65**, 36104 (2002)
4. C. Fraser, S. Riley, R.M. Anderson, N.M. Ferguson, Proc. Natl. Acad. Sci. **101**, 6146 (2004)
5. M. Camitz, F. Liljeros, BMC Medicine **4**, 32 (2006)
6. I.Z. Kiss, D.M. Green, R.R. Kao, J. R. Soc. Interface **3**, 55 (2006)
7. Y. Chen, G. Paul, S. Havlin, F. Liljeros, H.E. Stanley, Phys. Rev. Lett. **101**, 58701 (2008)
8. Shunjiang Ni, Wenguo Weng, Phys. Rev. E **79**, 016111 (2009)
9. L.B. Shaw, I.B. Schwartz, Phys. Rev. E **81**, 046120 (2010)
10. P. Bajardi, C. Poletto, J.J. Ramasco, M. Tizzoni, V. Colizza, A. Vespignani, PLoS ONE **6**, e16591 (2011)
11. L. Cao, X. Li, B. Wang, K. Aihara, Phys. Rev. E **84**, 041936 (2011)
12. S. Meloni, N. Perra, A. Arenas, S. Gómez, Y. Moreno, A. Vespignani, Sci. Rep. **1**, 62 (2011)
13. H.-F. Zhang, Z.-X. Wu, X.-K. Xu, M. Small, L. Wang, B.-H. Wang, Phys. Rev. E **88**, 012813 (2013)
14. L. Wang, Z. Wang, Y. Zhang, X. Li, Sci. Rep. **3**, 1468 (2013)
15. L. Wang, Y. Zhang, Z. Wang, X. Li, Int. J. Bifur. Chaos **23**, 1350095 (2013)
16. C.-Y. Xia, Z. Wang, J. Sanz, S. Meloni, Y. Moreno, Physica A **392**, 1577 (2013)
17. Z. Wang, H. Zhang, Z. Wang, Chaos Solitons Fractals **61**, 1 (2014)
18. S. Funk, M. Salathé, V.A.A. Jansen, J. R. Soc. Interface **7**, 1247 (2010)
19. S. Funk, E. Gilad, C. Watkins, V.A.A. Jansen, Proc. Natl. Acad. Sci. **106**, 6872 (2009)
20. P. Poletti, B. Caprile, M. Ajelli, A. Pugliese, S. Merler, J. Theor. Biol. **260**, 31 (2009)

21. S. Funk, E. Gilad, V.A.A. Jansen, J. Theor. Biol. **264**, 501 (2010)
22. N. Perra, D. Balcan, B. Gonçalves, A. Vespignani, PLoS ONE **6**, e23084 (2011)
23. P. Poletti, M. Ajelli, S. Merler, PLoS ONE **6**, e16460 (2011)
24. H. Zhang, J. Zhang, P. Li, M. Small, B. Wang, Physica D **240**, 943 (2011)
25. P. Poletti, M. Ajelli, S. Merler, Math. Biosci. **238**, 80 (2012)
26. T. Gross, C. D'Lima, B. Blasius, Phys. Rev. Lett. **96**, 208701 (2006)
27. D.H. Zanette, S. Risau-Gusmán, J. Biol. Phys. **34**, 135 (2008)
28. L.B. Shaw, I.B. Schwartz, Phys. Rev. E **77**, 066101 (2008)
29. S. Risau-Gusman, D.H. Zanette, J. Theor. Biol. **257**, 52 (2009)
30. S. Van Segbroeck, F.C. Santos, J.M. Pacheco, PLoS Comput. Biol. **6**, e1000895 (2010)
31. B. Wang, L. Cao, H. Suzuki, K. Aihara, J. Phys. A **44**, 035101 (2011)
32. S.V. Segbroeck, F.C. Santos, T. Lenaerts, J.M. Pacheco, New J. Phys. **13**, 013007 (2011)
33. E.P. Fenichel et al., Proc. Natl. Acad. Sci. **108**, 6306 (2011)
34. S. Wieland, T. Aquino, A. Nunes, Europhys. Lett. **97**, 18003 (2012)
35. P. Van Mieghem, R. Van de Bovenkamp, Phys. Rev. Lett. **110**, 108701 (2013)
36. M. Perc, A. Szolnoki, BioSystems **99**, 109 (2010)
37. L. Cao, H. Ohtsuki, B. Wang, K. Aihara, J. Theor. Biol. **272**, 8 (2011)
38. Z. Wang, Y. Liu, L. Wang, Y. Zhang, Z. Wang, Sci. Rep. **4**, 3597 (2014)
39. Zhen Wang, Lin Wang, Matjaž Perc, Phys. Rev. E **89**, 052813 (2014)
40. A. Lindgren, A. Doria, O. Schelén, Proc. ACM SigMobile **7**, 19 (2003)
41. J. Burgess, B. Gallagher, D. Jensen, B.N. Levine, Proc. IEEE Infocom. **6**, 1 (2006)
42. X. Zhang, G. Neglia, J. Kurose, D. Towsley, Comput. Networks **51**, 2867 (2007)
43. P. Erdős, A. Rényi, Acta Math. Hungarica **12**, 261 (1961)
44. R. Pastor-Satorras, A. Vespignani, Phys. Rev. E **63**, 066117 (2001)
45. B. Wang, L. Cao, H. Suzuki, K. Aihara, Sci. Rep. **2**, 887 (2012)
46. J. Wallinga, P. Teunis, Am. J. Epidemiol. **160**, 509 (2004)
47. A.L. Barabási, R. Albert, Science **286**, 509 (1999)
48. R. Pastor-Satorras, A. Vespignani, Phys. Rev. Lett. **86**, 3200 (2001)
49. R. Pastor-Satorras, A. Vespignani, Phys. Rev. E **65**, 036104 (2002)